Applied Catalysis B: Environmental 154–155 (2014) 171–176

Contents lists available at ScienceDirect

Applied Catalysis B: Environmental

journal homepage: www.elsevier.com/locate/apcatb

Catalytic activity of Pt/SiO_2 nanocatalysts synthesized via ultrasonic spray pyrolysis process under CO oxidation

Chan-Ho Jung[a,b], Jaecheol Yun[c], Kamran Qadir[a,b], Brundabana Naik[a,b], Jung-Yeul Yun[c,**], Jeong Young Park[a,b,*]

[a] Center for Nanomaterials and Chemical Reactions, Institute for Basic Science, Daejeon 305-701, Republic of Korea
[b] Graduate School of EEWS, Korea Advanced Institute of Science and Technology (KAIST), Daejeon 305-701, Republic of Korea
[c] Powder Technology Department, Korea Institute of Materials Science (KIMS), Chang won 641-831, Republic of Korea

ARTICLE INFO

Article history:
Received 19 November 2013
Received in revised form 2 February 2014
Accepted 8 February 2014
Available online 18 February 2014

Keywords:
Spray pyrolysis
Pt nanoparticles
Nanocatalyst
CO oxidation

ABSTRACT

We report the catalytic activity of Pt/SiO_2 nanocatalysts synthesized via the ultrasonic spray pyrolysis (USP) process under CO oxidation. We found that the average particle size of the dispersed platinum nanoparticles can be controlled by changing the concentration of the Pt precursor and the calcination conditions. The amount of loaded platinum on the SiO_2 powder increased as the precursor concentration increased, while the specific surface area of the Pt/SiO_2 samples decreased. As the calcination temperature and time increased, the size of the platinum particles on the SiO_2 increased. As for catalytic reactivity, high loading of Pt/SiO_2 showed a higher conversion of CO. The turnover rate of the Pt/SiO_2 catalysts increased after calcination at 600 °C, then decreased after calcination at 750 °C, mainly due to agglomeration at the high temperature and partly because of severe oxidation. The catalytic activity of the Pt/SiO_2 nanocatalysts synthesized using USP exhibited higher catalytic activity compared with Pt/SiO_2 synthesized via wet chemical synthesis or wetness impregnation. It is attributed to better dispersion of the nanoparticles on the SiO_2 as well as the removal of hydrocarbon impurities during calcination. This work demonstrated the successful use of the spray pyrolysis process for synthesis of oxide-supported metal catalysts with high thermal stability and activity.

1. Introduction

Metal-supported oxide hybrid catalysts show much promise in heterogeneous catalysis due to possible synergistic effects on catalytic activity due to metal-support interactions [1–5]. Particularly, various Pt nanoparticle-supported oxide systems have been extensively used for CO oxidation reactions during the past few decades, focusing on the metal-oxide interface [6–13]. The synthesis of model catalysts usually involves wet chemical routes (e.g., sol–gel, co-precipitation, deposition precipitation) where the organic capping agent or surfactant enables the catalytic nanoparticles to be tailor-made with tunable size, shape, and composition [14–17]. However, these colloid nanoparticles have low thermal stability above 300 °C and cannot maintain a pristine structure when the capping agent or surfactant decomposes at high temperature. Therefore, high-temperature reactions, such as CO oxidation [18], partial oxidation [19], hydrocarbon cracking [20], combustion [21], and ignition behavior studies [22] are not suitable for colloidal nanoparticles. Furthermore, these methods are time consuming, and not scalable up to large quantities. Hence, for large-scale synthesis, physical methods have an advantage over chemical techniques. The physical methods utilized by the catalysis community include spray pyrolysis [23], laser ablation [24], vapor deposition [25], and electrical wire explosion [26]. Considering the demand for rapid and large-scale synthesis of supported metal catalysts, the spray pyrolysis process appears to be a promising method to produce nanomaterials with new properties.

Among various methods to achieve precursor nebulization, the ultrasonic spray pyrolysis (USP) nebulizer is preferred because of its excellent energy efficiency in aerosol generation, inherently low velocity of the initial aerosol, and high affordability. It offers great flexibility for continuous flow processes that potentially synthesize desired nanomaterials at a large scale. During synthesis,

* Corresponding authors at: Institute for Basic Science, Center for Nanomaterials and Chemical Reactions, Daejeon 305-701, Republic of Korea. Tel.: +82 42 350 1713; fax: +82 42 350 1710.
** Corresponding authors at: Powder Technology Department, Korea Institute of Materials Science (KIMS), Changwon 642-831, Republic of Korea.
Tel.: +82 55 280 3561; fax: +82 55 280 3289.
E-mail addresses: yjy1706@kims.re.kr (J.-Y. Yun), jeongypark@kaist.ac.kr (J.Y. Park).

http://dx.doi.org/10.1016/j.apcatb.2014.02.014
0926-3373/

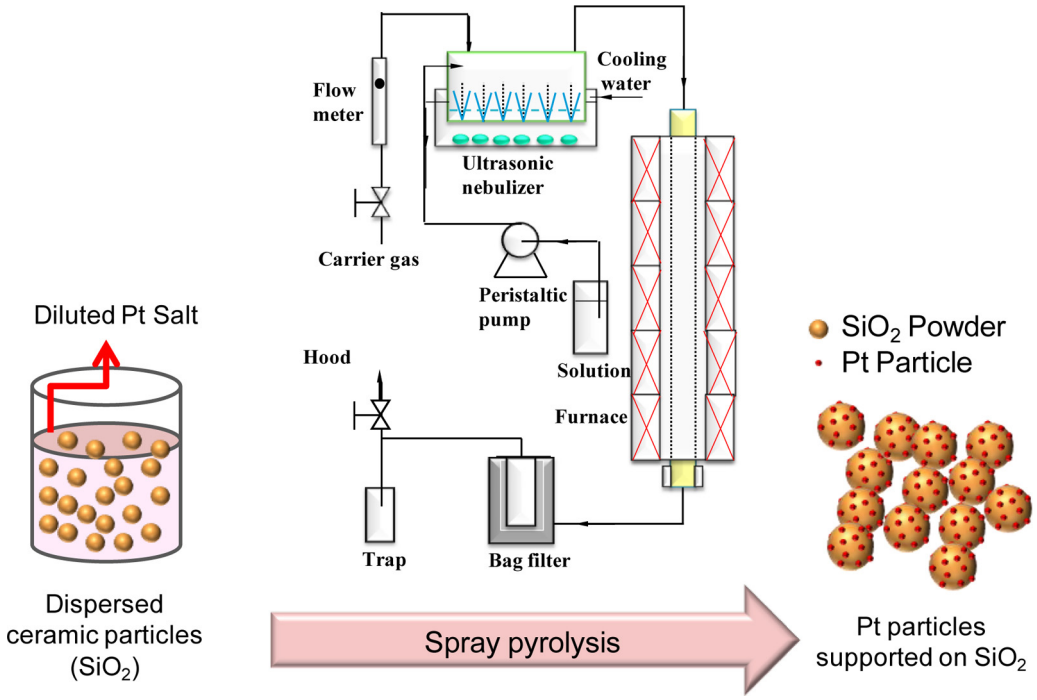

Fig. 1. Schematic diagram of the spray pyrolysis process for fabricating Pt/SiO_2 nanocatalysts.

atomized droplets of a precursor solution undergo evaporation and shrinkage while continuously flowing through a high-temperature reactor. By tuning the conditions, various types of desired hybrid nanocatalytic systems can be designed. Due to its simplicity, reproducibility, versatility, and low-cost, USP is a preferred industrial process [27]. USP fabricated metal supported oxides or nanocomposites have been thoroughly investigated throughout last decade and their catalytic application in photocatalysis [28–30], fuel cells [31], CO_2 hydrogenation [32], and hydrodesulfirization [33] have been highlighted. However, the reports on the CO oxidation reaction are rather scarce. Previously, Cu–Mn oxides synthesized via the spray pyrolysis method were evaluated for catalytic CO oxidation in a flow reactor [34]. The higher activity was attributed to spinnel structures with higher surface areas and more active sites. Fan et al. prepared Au–TiO_2 using the solution spray reaction and investigated the CO oxidation [35]. High dispersion of the Au and the strong metal support interaction effect are the key parameters for the high catalytic activity.

We prepared a series of Pt/SiO_2 catalysts by varying the Pt deposition concentration and calcination conditions, and studied them using the CO oxidation reaction. The structural and physicochemical properties were measured to study correlations with the catalytic activity of the nanocatalysts.

2. Experimental details

2.1. Catalyst fabrication

Pt/SiO_2 nanocatalyst powders with varying Pt content were fabricated using the spray pyrolysis method. Chloroplatinic acid hexahydrate ($H_2Cl_6Pt{\cdot}6H_2O$, Aldrich) and fumed silica (SiO_2, Aldrich) were used as the Pt precursor and support, respectively. The spray solutions were prepared by mixing SiO_2 dispersed in distilled water and aqueous solution of $H_2Cl_6Pt{\cdot}6H_2O$. To investigate different Pt contents, we fixed the amount of SiO_2 at 1 wt% of the spray solutions and varied the concentration of the $H_2Cl_6Pt{\cdot}6H_2O$ aqueous solution. The nebulizer used to make droplets consisted of 21 ultrasonic spray generators operating at 1.7 MHz. The droplets formed by the nebulizer were transferred to a tubular quartz reactor (length: 1000 mm; ID: 100 mm) at 500 °C and a flow rate of 50 l/min using air as the carrier gas. The Pt/SiO_2 nanocatalyst powder was obtained from a bag filter. The particle formation mechanism for the Pt/SiO_2 nanocatalyst powder synthesized by the spray pyrolysis process is shown in Fig. 1.

2.2. Catalyst and catalytic reaction characterization

We used inductively coupled plasma mass spectroscopy (ICP-MS; Perkin Elmer, DRC-e model) to measure Pt loading. The active area of the samples was obtained using CO pulse chemisorption (BELCAT-B; BEL Japan Inc.). Pretreatment was done at 400 °C under O_2 flow (50 sccm) for 15 min and H_2 flow (50 sccm) for 15 min. 10% CO gas balanced with He was used for the gas pulse; measurement was carried out at 50 °C. CO oxidation was performed with the nanocatalyst samples in a flow reactor [7]. Before the reaction, about 100 mg of catalyst was pelletized and loaded in a quartz tube. Subsequently, the catalyst was reduced at 250 °C under H_2 flow (5% H_2 in He, a flow of 45 ml/min) for 30 min, and then cooled to room temperature. The reactant gas composition was 4% CO, 10% O_2, and 86% He (balance). The total gas flow rate was 50 ml/min, controlled by mass flow controllers (BROOKS instrument). The space velocity of the reaction (GHSV) was 15,000 h^{-1}. CO oxidation was carried out until 100% CO conversion (in the temperature range of 100–240 °C). The gas mixture passing through the catalyst powder was analyzed using gas chromatography (GC; DS science).

3. Results and discussion

Fig. 2 shows the size distribution of the Pt nanoparticles dispersed on SiO_2 after attachment and after aging heat treatment using the Pt/SiO_2 nanocatalyst powder, which had a Pt content of 4 wt%. To improve adhesion between the Pt nanoparticles and the SiO_2 particles, heat treatment was carried out at 600 °C for 30 min under atmospheric gas conditions (Fig. 2a). The size of the Pt nanoparticles was measured using TEM images; the Pt nanoparticles showed a mean size of 8.4 nm (Fig. 2c). To investigate the effect

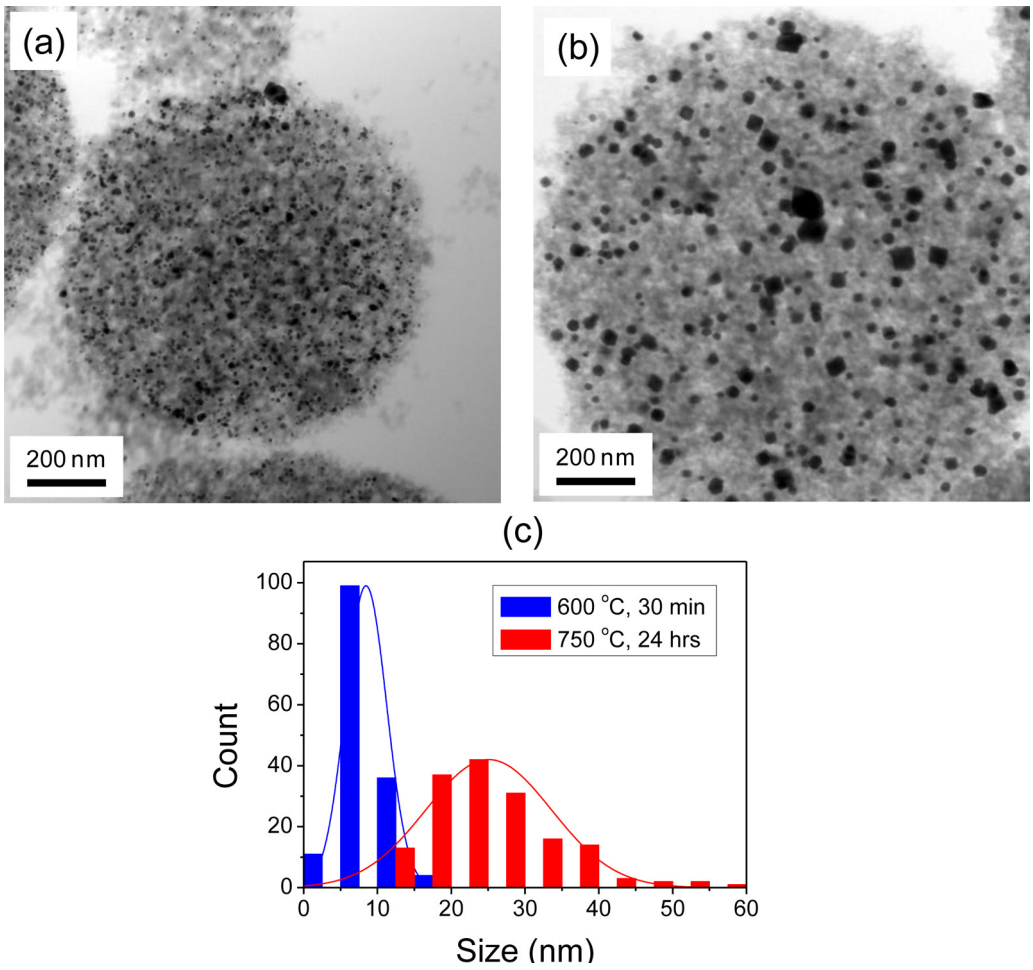

Fig. 2. TEM images of Pt/SiO_2 (4 wt% Pt) nanocatalysts (a) calcined at 600 °C for 30 min and (b) calcined at 750 °C for 24 h. (c) Size distribution histograms of Pt/SiO_2 (4 wt% Pt) nanocatalysts calcined at two different conditions (600 °C for 30 min and 750 °C for 24 h), showing the effect of sintering after high-temperature calcination.

of aging on the catalysts, heat treatment of the Pt/SiO_2 nanocatalyst powder was performed for 24 h at 750 °C under atmospheric conditions. The Pt nanoparticles were larger following the aging heat treatment (Fig. 2b) due to sintering of the Pt nanoparticles. The mean size of the Pt nanoparticles after the aging heat treatment was 26 nm (Fig. 2c).

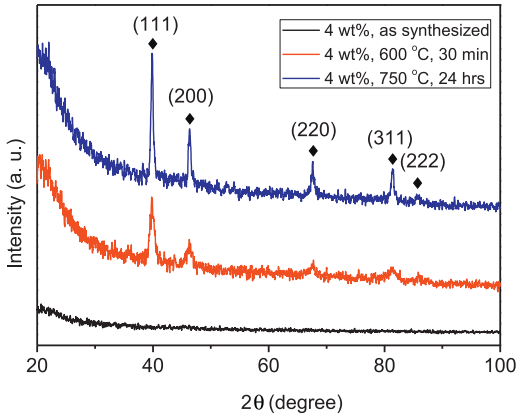

Fig. 3. XRD patterns of Pt/SiO_2 (4 wt%) samples with three different treatments: as synthesized, after calcination at 600 °C for 30 min, and after calcination at 750 °C for 24 h.

Fig. 3 shows the XRD results of the Pt/SiO_2 (4 wt% Pt) nanocatalyst powders. The precursor powders synthesized via the spray pyrolysis method only showed an amorphous structure and the Pt phases were not observed because the short residence time for droplet transfer did not provide sufficient time for nucleation and growth of the Pt nanoparticles. After attachment heat treatment, the Pt phase with peaks of (1 1 1), (2 0 0), (2 2 0), (3 1 1), and (2 2 2) was observed (Fig. 3). The peak intensity of the Pt nanoparticles increased due to sintering of the nanoparticles after heat treatment (Fig. 3). Table 1 shows the chemisorption results for the samples, which were measured by CO pulse chemisorption. Metal dispersion increased and the metal surface area decreased as the Pt loading increased. In the case of calcination, both the metal dispersion and metal surface area decreased as the calcination temperature and time increased. The average particle diameter increased as the Pt loading and calcination temperature increased.

XPS data were collected for the Pt/SiO_2 (4 wt%) samples with three different treatments, as shown in Fig. 4, as synthesized, after calcination at 600 °C for 30 min, and after calcination at 750 °C for 24 h. We observed two oxidation states of Pt: 2+ and 4+ (i.e., PtO and PtO_2, respectively). The chemical shifts of the Pt 4f core level of the PtO and PtO_2 relative to pure Pt are about 1.2 and 3.0 eV, respectively, which is consistent with earlier work on Pt nanoparticles [8,12].

Fig. 5 shows the CO conversion rate of the Pt/SiO_2 nanocatalysts for two different loadings, (a) 1 wt% and (b) 4 wt%, with three different treatments: as synthesized, after calcination at 600 °C for

Table 1
Chemisorption results, T_{100}, and activation energies of the Pt/SiO_2 samples.

	1 wt%, as synthesized	1 wt%, 600 °C, 30 min	1 wt%, 750 °C, 24 h	4 wt%, as synthesized	4 wt%, 600 °C, 30 min	4 wt%, 750 °C, 24 h
Metal dispersion (%)	40.85	2.97	0.54	21.23	5.27	0.39
Metal surface area per sample weight (m^2/g)	1.01	0.07	0.01	2.62	0.65	0.05
T_{100} (°C)	200	215	270	180	190	240
Activation energy (kcal/mol)	19.54	30.87	27.16	19.60	21.74	32.15

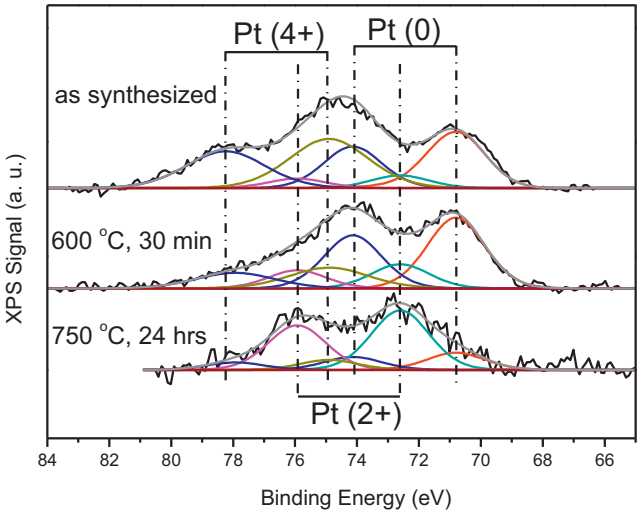

Fig. 4. XPS data of Pt/SiO_2 (4 wt%) samples with three different treatments: as synthesized, after calcination at 600 °C for 30 min, and after calcination at 750 °C for 24 h. Because the samples were not reduced, the XPS data show mild oxidation states of Pt, which depend on the calcination conditions.

30 min, and after calcination at 750 °C for 24 h. The temperature at 100% CO conversion (T_{100}) for 1 wt% Pt/SiO_2 was 200 °C for the as-synthesized Pt/SiO_2, 215 °C for Pt/SiO_2 calcined at 600 °C for 30 min, and 270 °C for Pt/SiO_2 calcined at 750 °C 24 h, as shown in Fig. 5(a). The T_{100} for 4 wt% Pt/SiO_2 was 180 °C for the as-synthesized Pt/SiO_2, 190 °C for Pt/SiO_2 calcined at 600 °C for 30 min, and 240 °C for Pt/SiO_2 calcined at 750 °C for 24 h (Fig. 5(b)). As shown in Fig. 5, CO conversion rates exhibits the abrupt jump from 30% to 100%, that is related to ignition of CO oxidation. In ignition, the high rate of CO_2 production causes a rapid increase in temperature. It takes place when the heat losses in the catalysts can no longer keep pace with the amount of chemical energy evolved by the exothermic chemical reactions [36]. General trends are that the overall CO conversion efficiency is proportional to the Pt loading. The 4 wt% loaded sample exhibited a lower conversion temperature, compared with the 1 wt% loaded sample, due to the higher surface area. After heating at 750 °C for 24 h, both the 1 wt% and 4 wt% loaded sample had higher conversion temperatures, which is associated with nanoparticle sintering, as is confirmed in the TEM images.

Fig. 6a shows the turnover rate of the six samples with different loading and treatment temperatures. We calculated the turnover frequency using the Pt active sites obtained by chemisorptions and CO conversion data obtained by the oxidation reaction via the flow reactor. The turnover rate of CO oxidation is given by

$$\mathrm{TOF} = \frac{[\text{number of oxidized CO molecules}]}{[\text{number of active surface Pt atoms}]}, \quad (1)$$

where [number of active Pt molecules] = [metal surface area (m^2/g)] × [sample weight (g)] × atomic density of Pt surface ($1.3 \times 10^{19}\ m^{-2}$)], and [number of oxidized CO molecules] is calculated using the ideal gas equation (PV = nRT, P = gas pressure (2 atm), V = flow rate (2.0 ml/min), R = gas constant (0.082 atm l/K mol)).

According to the corresponding Arrhenius plot (Fig. 6b), the Pt/SiO_2 calcined at 600 °C for 30 min showed the highest turnover rate. Some hydrocarbon impurities on the Pt precursors possibly exist on the surface of the nanoparticles. Calcination can remove these hydrocarbon impurities, resulting in improved catalytic activity. However, in the case of Pt/SiO_2 calcined at 750 °C for 24 h, sintering caused deactivation of the nanoparticles. According to the TEM images, the platinum particles were well dispersed on the silica substrate with a low particle size (around 5 nm) with a narrow size distribution, whereas the Pt/SiO_2 calcined at 750 °C showed a larger particle size (around 25 nm) with a broad size distribution. Also, the higher oxidation states observed on the Pt/SiO_2 calcined at 750 °C for 24 h (shown in Fig. 4) are partly responsible for the lower catalytic activity.

The catalytic activity of the Pt/SiO_2 nanocatalysts synthesized via spray pyrolysis exhibited higher catalytic activity compared with Pt/SiO_2 synthesized using wet chemical synthesis or wetness impregnation. For example, at 200 °C, we obtained a turnover frequency of 1.4 s^{-1} for the 1 wt% catalyst sample calcined at 600 °C

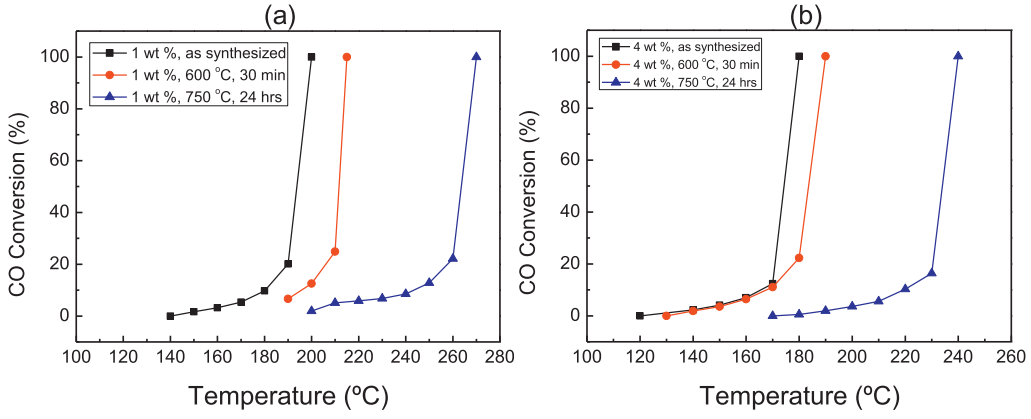

Fig. 5. CO conversion for the Pt/SiO_2 samples ((a) 1 wt%, and (b) 4 wt%) with three different treatments: as synthesized, after calcination at 600 °C for 30 min, and after calcination at 750 °C for 24 h.

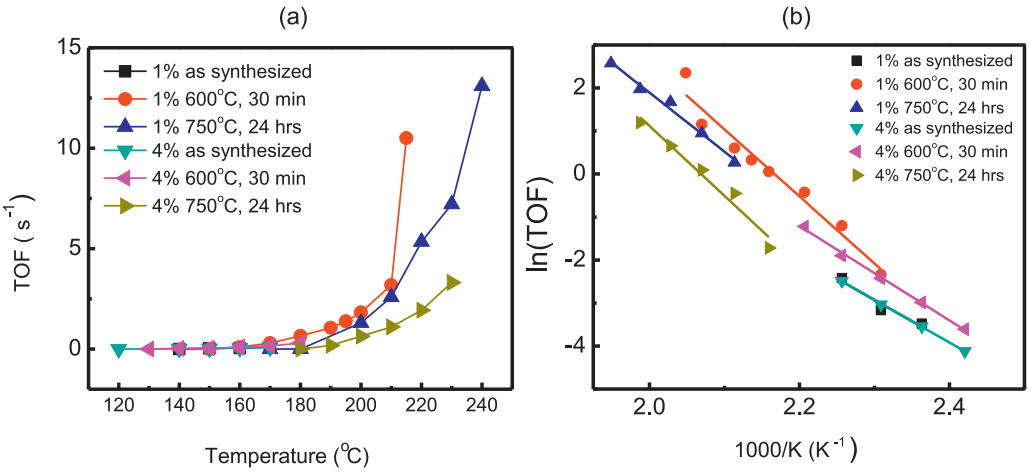

Fig. 6. (a) Turnover rate plot for the Pt/SiO_2 catalysts treated at different temperatures. (b) Arrhenius plot for the Pt/SiO_2 catalysts.

for 30 min, which is higher than that of the Pt/SBA-15 catalyst synthesized using wetness impregnation ($0.06\ s^{-1}$) or Pt/SiO_2 catalyst synthesized via wet chemical synthesis ($0.1\ s^{-1}$) [37,38]. We attribute this to better dispersion of the nanoparticles on the SiO_2 as well as the absence of hydrocarbon contamination, demonstrating a clear advantage of fabricating nanocatalysts using spray pyrolysis. In USP, ultrasound nebulizes the precursor solution to produce micro-sized droplets that acts as isolated, individual microreactors. Thus, micro-sized silica spheres with high dispersion of Pt nanoparticles can be formed, as confirmed by TEM measurements. In fact, a distinctive feature of the resulting products obtained via the USP method is the homogeneous distribution of constituents throughout all the particles because all of the constituents are formed from a solution [39]. Moreover, it is proven that the presence of additional components during synthesis of metal oxides through USP strengthen the thermal stability of the product [40]. As we have incorporated Pt precursor during synthesis, the Pt-SiO_2 catalysts have high thermal stability, which is one of the key parameters in the CO oxidation reaction. Therefore, spray pyrolysis may provide large-scale synthesis of reactive catalysts for industrial applications.

4. Conclusion

In conclusion, a catalytically active Pt/SiO_2 powder was fabricated via the spray pyrolysis process. TEM, XRD, and chemisorption instruments were used to measure the morphology, metal nanoparticle size distribution, and active area of the Pt/SiO_2 powders, respectively. Using spray pyrolysis, the catalyst nanoparticles (with an average particle size of 8.45 nm) were well dispersed on the SiO_2 powder. Accordingly, the amount of platinum loaded on the SiO_2 powder increased, but the specific surface area of the Pt/SiO_2 samples decreased. As for catalytic reactivity, the Pt/SiO_2 sample with higher platinum loading showed a lower T_{100}. The catalytic activity of CO oxidation was affected by calcination temperature and time; Pt/SiO_2 calcined at 600 °C for 30 min showed the highest catalytic activity.

Acknowledgments

The work was supported by the Institute for Basic Science (IBS) [CA1401-04] and by a grant from the Fundamental R&D Program for Core Technology of Materials funded by the Ministry of Trade, Industry & Energy, Republic of Korea.

References

[1] G.A. Somorjai, J.Y. Park, Angewandte Chemie International Edition 47 (2008) 9212.
[2] M. Haruta, N. Yamada, T. Kobayashi, S. Iijima, Journal of Catalysis 115 (1989) 301.
[3] K. Hayek, M. Fuchs, B. Klötzer, W. Reichl, G. Rupprechter, Topics in Catalysis 13 (2000) 55.
[4] S.J. Tauster, Accounts of Chemical Research 20 (1987) 389.
[5] S.J. Tauster, S.C. Fung, Journal of Catalysis 55 (1978) 29.
[6] A.S. Reddy, S. Kim, H.Y. Jeong, S. Jin, K. Qadir, K. Jung, C.H. Jung, J.Y. Yun, J.Y. Cheon, J.-M. Yang, S.H. Joo, O. Terasaki, J.Y. Park, Chemical Communications 47 (2011) 8412.
[7] S.H. Kim, C.-H. Jung, N. Sahu, D. Park, J.Y. Yun, H. Ha, J.Y. Park, Applied Catalysis A: General 454 (2013) 53.
[8] J. Park, C. Aliaga, J.R. Renzas, H. Lee, G. Somorjai, Catalysis Letters 129 (2009) 1.
[9] J.Y. Park, Y. Zhang, M. Grass, T. Zhang, G.A. Somorjai, Nano Letters 8 (2008) 673.
[10] M. Graham, M. Bär, I. Kevrekidis, K. Asakura, J. Lauterbach, H.-H. Rotermund, G. Ertl, Physical Review E: Statistical, Nonlinear, and Soft Matter Physics 52 (1995) 76.
[11] J. Oi-Uchisawa, A. Obuchi, R. Enomoto, A. Ogata, S. Kushiyama, Chemical Communications (1998) 2255.
[12] K. Qadir, S.H. Kim, S.M. Kim, H. Ha, J.Y. Park, Journal of Physical Chemistry C 116 (2012) 24054.
[13] X. Zhu, H. Zhang, Y. Zhang, Y. Liang, X. Yang, B. Yi, Journal of Physical Chemistry B 110 (2006) 14240.
[14] G.A. Somorjai, J.Y. Park, Topics in Catalysis 49 (2008) 126.
[15] P. Yang, D. Zhao, D.I. Margolese, B.F. Chmelka, G.D. Stucky, Nature 396 (1998) 152.
[16] P.T. Tanev, M. Chibwe, T.J. Pinnavaia, Nature 368 (1994) 321.
[17] C. Kresge, M. Leonowicz, W. Roth, J. Vartuli, J. Beck, Nature 359 (1992) 710.
[18] M. Kim, M. Bertram, M. Pollmann, A.v. Oertzen, A.S. Mikhailov, H.H. Rotermund, G. Ertl, Science 292 (2001) 1357.
[19] A. Ashcroft, A. Cheetham, M. Green, Nature 352 (1991) 225.
[20] E.D. Bloch, W.L. Queen, R. Krishna, J.M. Zadrozny, C.M. Brown, J.R. Long, Science 335 (2012) 1606.
[21] M. Mapa, C.S. Gopinath, Chemistry of Materials 21 (2008) 351.
[22] S.H. Joo, J.Y. Park, C.-K. Tsung, Y. Yamada, P. Yang, G.A. Somorjai, Nature Materials 8 (2009) 126.
[23] W.H. Suh, K.S. Suslick, Journal of the American Chemical Society 127 (2005) 12007.
[24] A.M. Morales, C.M. Lieber, Science 279 (1998) 208.
[25] K. Okano, S. Koizumi, S.R.P. Silva, G.A. Amaratunga, Nature 381 (1996) 140.
[26] J.Y. Yun, A.S. Reddy, S. Yang, H.J. Kim, H.Y. Koo, H.M. Lee, C.H. Jung, K. Qadir, S. Kim, J.Y. Park, Catalysis Letters 142 (2012) 326.
[27] R. Mueller, L. Mädler, S.E. Pratsinis, Chemical Engineering Science 58 (2003) 1969.
[28] Y. Huang, Z. Zheng, Z. Ai, L. Zhang, X. Fan, Z. Zou, The Journal of Physical Chemistry B 110 (2006) 19323.
[29] Y. Huang, Z. Ai, W. Ho, M. Chen, S. Lee, The Journal of Physical Chemistry C 114 (2010) 6342.
[30] J.H. Bang, R.J. Helmich, K.S. Suslick, Advanced Materials 20 (2008) 2599.
[31] J.H. Bang, K. Han, S.E. Skrabalak, H. Kim, K.S. Suslick, The Journal of Physical Chemistry C 111 (2007) 10959.

[32] D. Li, N. Ichikuni, S. Shimazu, T. Uematsu, Applied Catalysis A: General 180 (1999) 227.
[33] S.E. Skrabalak, K.S. Suslick, Journal of the American Chemical Society 127 (2005) 9990.
[34] G. Fortunato, H.R. Oswald, A. Reller, Journal of Materials Chemistry 11 (2001) 905.
[35] L. Fan, N. Ichikuni, S. Shimazu, T. Uematsu, Applied Catalysis A: General 246 (2003) 87.
[36] K.R. McCrea, J.S. Parker, G.A. Somorjai, Journal of Physical Chemistry B 106 (2002) 10854.
[37] A.K. Prashar, S. Mayadevi, P.R. Rajamohanan, R. Nandini Devi, Applied Catalysis A: General 403 (2011) 91.
[38] J.N. Kuhn, C.-K. Tsung, W. Huang, G.A. Somorjai, Journal of Catalysis 265 (2009) 209.
[39] J.H. Bang, K.S. Suslick, Advanced Materials 22 (2010) 1039.
[40] B. Xia, I.W. Lenggoro, K. Okuyama, Advanced Materials 13 (2001) 1579.